GEOPHYSICAL RESEARCH LETTERS, VOL. 23, NO. 22, PAGES 3207-3210, NOVEMBER 1, 1996

Polar vortex conditions during the 1995–96 Arctic winter: MLS ClO and HNO_3

M. L. Santee, G. L. Manney, W. G. Read, L. Froidevaux, and J. W. Waters

Jet Propulsion Laboratory, California Institute of Technology, Pasadena

Abstract. Microwave Limb Sounder (MLS) measurements of lower stratospheric ClO and HNO_3 during the 1995–96 Arctic winter are presented. The 1995–96 Arctic winter was both colder and more persistently cold than usual, leading to an enhancement in lower stratospheric ClO of greater magnitude, vertical extent, and duration than previously observed in the Arctic. Vortex concentrations of HNO_3 in mid-December were large due to diabatic descent. Trajectory calculations indicate that localized severe depletions of gas-phase HNO_3 in mid-February and early March did not arise from entrainment of midlatitude air into the vortex and were therefore probably related to polar stratospheric cloud (PSC) formation. A strong correlation between temperature and gas-phase HNO_3 was evident, consistent with recurring PSC condensation and evaporation cycles.

Introduction

Significant interhemispheric differences in the severity of ozone depletion are attributed in large measure to underlying differences in seasonal temperature patterns and vortex behavior [*World Meteorological Organization (WMO)*, 1995]. The 1995–96 Arctic winter was both colder and more persistently cold than usual. Two upper tropospheric blocking ridges led to lower stratospheric minimum temperatures that approached those of the Antarctic vortex. The 1995–96 Arctic winter meteorological conditions, and their influence on ozone destruction, are discussed by *Manney et al.* [1996a].

In this paper we examine the 1995–96 Arctic winter temperatures in relation to chlorine activation and the formation of PSCs. Only a limited number of direct satellite observations of PSCs were obtained inside the 1995–96 Arctic vortex from the Polar Ozone and Aerosol Measurement (POAM) II and the Upper Atmosphere Research Satellite (UARS) Halogen Occultation Experiment (HALOE). However, gas-phase HNO_3 is now being obtained in the lower stratosphere with daily hemispheric coverage from UARS MLS measurements and is used here to infer the presence of PSCs.

Measurement Description

UARS MLS observations of lower stratospheric ClO have been shown previously for several northern and southern hemisphere winters [*Waters et al.*, 1993a, b, 1995; *Manney et al.*, 1996b]. As reported by *Waters et al.* [1996], HNO_3 has a small effect on the ClO signal that was accounted for in the original retrieval algorithms by assuming climatological values. Version 3 ClO values were biased high by as much as 0.2 ppbv when HNO_3 departed substantially from climatology (e.g., under conditions of low gas-phase HNO_3 during PSC events). *Waters et al.* [1996] also report an 8% scaling error in the Version 3 ClO data arising from the use of an erroneous ClO line strength file. Both error sources have been corrected in improved retrieval algorithms. Here we present new Version 4 ClO data, which have an estimated single-profile precision and accuracy (see *Waters et al.* [1996] for an elaboration of these terms) of 0.4 ppbv and 10%, respectively, at 46 hPa.

The measurement of HNO_3 was not a primary MLS objective. However, there is a significant HNO_3 spectral feature, composed of many R-branch rotational lines, which resides just outside the 205-GHz spectral region used to measure ozone. In the lower stratosphere, the pressure-broadened line shape of this feature adds a weak slope to the ozone signal. Version 4 algorithms use this slope to retrieve profiles of gas-phase HNO_3, resulting in improved fits to the radiances. MLS HNO_3 measurements (from precursory algorithms) were first presented by *Santee et al.* [1995].

Preliminary validation studies indicate that the MLS HNO_3 data are scientifically useful on the 100, 46, and 22 hPa retrieval surfaces, where the estimated single-profile precisions are approximately 2.0, 3.0, and 4.5 ppbv, respectively. The estimated precisions are based on the observed variability in a narrow latitude band centered around the equator that was chosen to minimize the effects of natural atmospheric variability. Because the actual atmospheric variation is not completely negligible, the true precisions may be slightly better than these estimates. These empirical precisions are generally consistent with uncertainties derived theoretically from the measurement noise. The retrieval algorithm is based on sequential estimation and uses an a priori estimate from a month- and latitude-dependent climatology. When the contribution from the a priori to the retrieved values exceeds 25%, the uncertainties are flagged with a negative sign to signify poor measurement sensitivity. Thus quality control should be imposed on the HNO_3 data by discarding retrievals with negative uncertainty values.

Initial comparisons (over a limited data set) with colocated UARS Cryogenic Limb Array Etalon Spectrometer (CLAES) HNO_3 observations [*Kumer et al.*,

Paper number 96GL02454.
0094-8534/96/96GL-02454$05.00

1996] show that the MLS HNO_3 agrees well at 100 hPa but is usually 0-2 ppbv lower at 46 hPa and 0-4 ppbv higher at 22 hPa (particularly in the polar regions). However, even where biases between the two data sets exist, there is good correspondence in the morphology of the CLAES and MLS HNO_3 fields.

Analysis and Discussion

Maps of MLS ClO and gas-phase HNO_3 are presented in Fig. 1 for selected days during the two 1995–96 north-viewing winter periods. MLS data are gridded by binning and interpolating 24 hours of data, and interpolated to the 465 K potential temperature (θ) surface using United Kingdom Meteorological Office (UKMO) temperatures. Contours of temperature and potential vorticity (PV) derived from the UKMO analyses are also shown. After the second week of December, 465 K minimum temperatures remained at or below 195 K [*Manney et al.*, 1996a], the commonly-used threshold for the existence of Type I PSCs, until early March. Heterogeneous processing on PSC particles [e.g., *Solomon*, 1990] led to a substantial area of activated chlorine by mid-December; by late January, when north-viewing observations resumed, enhanced ClO filled most of the sunlit portion of the vortex.

Time series of vortex-averaged 465 K ClO are shown in Fig. 2 for the five northern winters of MLS measurements to date. To conserve instrument lifetime, full vertical scans were performed only on selected days in the 1994–95 and 1995–96 northern winters. ClO enhancement in late December 1995 was greater than that in any of the previous UARS years, although data were sparse at this time in 1994. Vortex-averaged ClO in February 1996 was as high as ever previously observed in the Arctic, and the ClO remained enhanced longer. Both Version 3 and Version 4 ClO data are shown for 1995–96. Although the vortex averages from both data sets exhibit the same time evolution, Version 3 values are larger due to the 8% line strength error and the contamination from HNO_3; as expected, the largest differences between the two versions occur on days for which gas-phase HNO_3 values are lowest (i.e., are furthest from climatological values, see previous section and *Waters et al.* [1996]).

Significant ClO enhancement extended up to ~650 K in 1995–96, as shown in Fig. 3. This exceeds the vertical range of enhanced ClO observed in previous Arctic winters (e.g., ClO was enhanced up to ~580 K in both 1992–93 [*Manney et al.*, 1994] and 1994–95 [*Manney et al.*, 1996b]). The larger vertical extent of the ClO enhancement in February 1996 is consistent with the larger vertical extent of both temperatures below 195 K and ozone depletion [*Manney et al.*, 1996a], and is similar to that typically seen in the Antarctic [*Manney et al.*, 1994].

High HNO_3 values in the vortex in mid-December (Fig. 1) are attributed to diabatic descent. Between 29 and 30 January, 465 K gas-phase HNO_3 increased by ~3.1 ppbv on average over northern Scandinavia. Temperatures over this region, while remaining below 195 K, increased by ~1.3 K during this interval. In light of recent studies that have called into question the canonical model of Type I PSC formation, we have used the thermodynamic formula of *Hanson and Mauersberger* [1988], along with the observed temperatures and an H_2O mixing ratio of 4.5 ppmv [*Kelly et al.*, 1990], to calculate the vapor pressure of HNO_3 over nitric acid trihydrate (NAT) at 46 hPa. We find that, although the observed increase in gas-phase HNO_3 is consistent with that predicted by the *Hanson and Mauersberger* [1988] relationship for the observed temperature increase, the MLS HNO_3 mixing ratios themselves are larger than those calculated over NAT for the same temperature.

A severe decrease in gas-phase HNO_3 occurred between 17 and 20 February, as temperatures dropped below 188 K between Greenland and Norway. The HNO_3 depletion extended up to 585 K and was confined to the area of low temperatures throughout its vertical range. As discussed by *Manney et al.* [1996a], a strong blocking ridge in the upper troposphere at this time resulted in the deformation of the lower stratospheric vortex and the location of a region of very low temperatures near the vortex edge (see Fig. 1). To investigate the cause of the HNO_3 decrease, high-resolution three-dimensional transport calculations, similar to those for ozone described by *Manney et al.* [1996a], were initialized using 465 K MLS HNO_3 on 30 January and run through 20 February. The trajectory calculations (Fig. 4a) do not show any cross-vortex transport of air parcels from regions where the HNO_3 mixing ratios were comparable to those observed in the cold vortex area, indicating that the localized HNO_3 depletion on 20 February (Fig. 1) did not arise from entrainment of lower-latitude air with smaller HNO_3 concentrations into the vortex associated with the tropospheric ridge. A second (weaker) tropospheric blocking event occurred at the beginning of March [*Manney et al.*, 1996a]. Another set of transport calculations was initialized on 24 February and run through 3 March. Again, the trajectory calculations (Fig. 4b) show that the low HNO_3 values observed on 3 March (Fig. 1) were not produced by intrusions of extra-vortex air during the second ridging event. High aerosol extinction indicative of PSCs was detected in the region where MLS measured low HNO_3 mixing ratios on 20 February and 3 March by POAM II (R. Bevilacqua, personal communication, 1996) and on 3 March by HALOE (J. Russell, personal communication, 1996). We conclude that the observed pockets of depleted gas-phase HNO_3 resulted from PSC formation.

The relationship between temperature and observed gas-phase HNO_3 is illustrated in Fig. 5 for the second north-viewing winter period. Area-weighted averages were calculated from points enclosed within the 195 K temperature contour. Because of the occasionally significant differences between UKMO and U. S. National Meteorological Center (NMC) lower stratospheric temperatures and the sensitivity of gas-phase HNO_3 mixing ratios to small temperature variations, the daily averages were computed using both UKMO and NMC temperatures. Similar results were obtained for both data sets. The strong correlation between temperature and

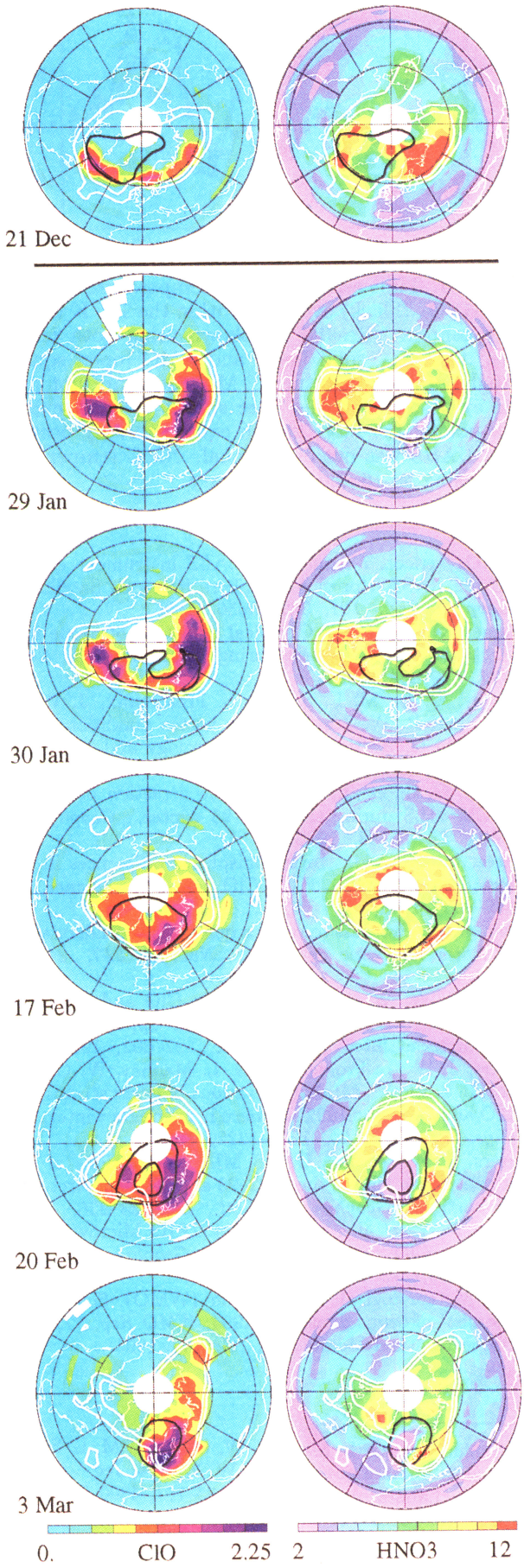

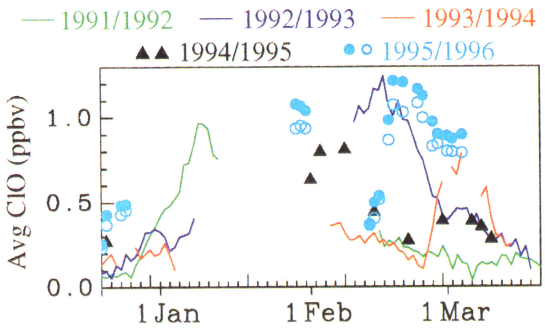

Figure 2. Time series of area-weighted vortex averages of 465 K ClO for five northern winters. Lack of measurements in daylight due to UARS orbit precession led to lower values of ClO in mid-February/early March each year. Large data gaps in January/early February occurred when MLS viewed southern high latitudes; the smaller gap in early February 1996 occurred when the UARS spacecraft was not operational. Both Version 3 (filled cyan circles) and Version 4 (open cyan circles) data are shown for 1995–96; for all other years the data shown are Version 3.

gas-phase HNO_3 suggests recurring PSC condensation and evaporation cycles. (A few apparent inconsistencies occur around days for which temperature is shown but no MLS data are available (e.g., 19–20 February) or the trends are small compared to the uncertainties (e.g., 23–24 February)). Further studies are in progress

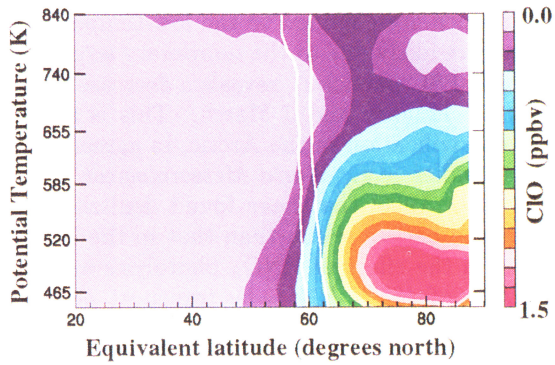

Figure 3. Version 4 ClO averaged over 18, 20 and 23 February (the days with highest 465 K ClO), in PV/θ space. PV is expressed as equivalent latitude (the latitude enclosing the same area as the PV contour). Two PV contours near the vortex edge (scaled to give similar values throughout the θ domain) are overlaid in white.

Figure 1. Maps of 465 K MLS ClO (left, ppbv) and HNO_3 (right, ppbv), for selected days during the two 1995–96 northern winter north-viewing periods. These are orthographic projections, with 0° longitude at the bottom and dashed black circles at 30°N and 60°N; blank spaces represent data gaps or spurious data points. Only data from the "day" side of the orbit are shown for ClO. Superimposed in white are the 0.25×10^{-4} and 0.30×10^{-4} $Km^2kg^{-1}s^{-1}$ UKMO PV contours (the approximate edge of the polar vortex) and in black the 195 and 188 K UKMO temperature contours (the approximate existence thresholds for Type I and Type II PSCs, respectively).

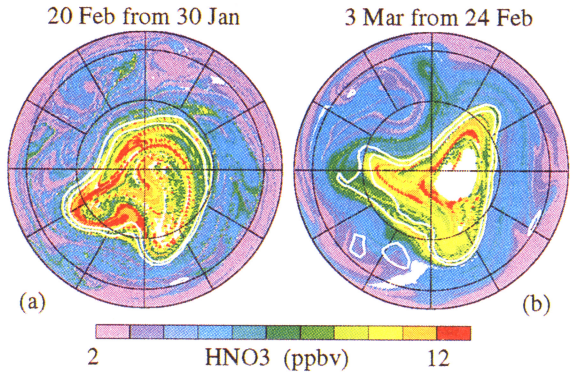

Figure 4. 465 K HNO_3 from high-resolution trajectory calculations [*Manney et al.*, 1996a]. Two PV contours (see Fig. 1) are overlaid in white. White spaces arise from data gaps in MLS HNO_3 on the initialization day. (a) Results on 20 February from calculations initialized on 30 January. (b) Results on 3 March from calculations initialized on 24 February.

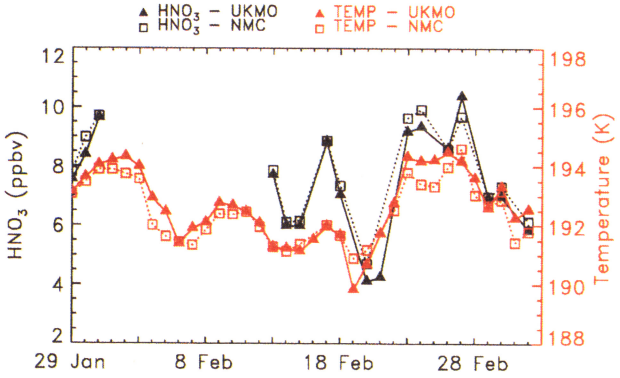

Figure 5. Time series of 465 K temperature (red) and MLS HNO_3 (black) averaged within the 195 K temperature contour. Results are shown using both UKMO (filled triangles, solid lines) and NMC (open squares, dotted lines) temperatures. MLS data are not available every day and the lines simply connect existing data points; the large gap in early February occurred when UARS was not operational. NMC temperatures are missing on 16 and 21 February.

to investigate how closely the behavior of MLS HNO_3 (and its correlation to temperature) conforms to that predicted by current models of PSC formation.

The MLS HNO_3 data alone do not allow us to distinguish between the temporary condensation of HNO_3 and the irreversible removal of HNO_3 through sedimentation of PSC particles (denitrification). However, Fig. 1 shows signs of an overall decline in gas-phase HNO_3 within the vortex over the course of the winter. Calculation of daily HNO_3 vortex averages, excluding regions where the mixing ratio was less than 4 ppbv (which are confined to the low-temperature regions and are likely due to the temporary sequestration of HNO_3 in PSC particles), reveals a decrease of 1 ppbv between 29 January and 3 March. This is suggestive of mild denitrification in the Arctic, in agreement with previous studies [e.g., *World Meteorological Organization (WMO)*, 1995] that have found denitrification in the Arctic to be less severe than that in the Antarctic. Modeling of the effect of HNO_3 photolysis and the replenishment of 465 K HNO_3 by transport processes is needed to verify this suggestion. The availability of a multi-year, global HNO_3 data set from MLS will facilitate more detailed comparisons of denitrification in the two hemispheres.

Acknowledgments. We thank our MLS colleagues, especially T. Lungu, L. Nakamura and R. P. Thurstans; the NMC and the UKMO for meteorological data; and C. Webster, M. Fromm and the reviewers for helpful comments. Work at the Jet Propulsion Laboratory, California Institute of Technology, was done under contract with the National Aeronautics and Space Administration.

References

Hanson, D., and K. Mauersberger, Laboratory studies of the nitric acid trihydrate: Implications for the south polar stratosphere, *Geophys. Res. Lett.*, *15*, 855–858, 1988.

Kelly, K. K., et al., A comparison of ER-2 measurements of stratospheric water vapor between the 1987 Antarctic and 1989 Arctic airborne missions, *Geophys. Res. Lett.*, *17*, 465–468, 1990.

Kumer, J. B., et al., Comparison of correlative data with HNO_3 version 7 from the CLAES instrument deployed on the NASA Upper Atmosphere Research Satellite, *J. Geophys. Res.*, *101*, 9621–9656, 1996.

Manney, G. L., et al., Chemical depletion of ozone in the Arctic lower stratosphere during winter 1992–93, *Nature*, *370*, 429–434, 1994.

Manney, G. L., M. L. Santee, L. Froidevaux, J. W. Waters, and R. W. Zurek, Polar vortex conditions during the 1995–96 Arctic winter: Meteorology and MLS ozone, *Geophys. Res. Lett.*, this issue, 1996a.

Manney, G. L., et al., Arctic ozone depletion observed by UARS MLS during the 1994–95 winter, *Geophys. Res. Lett.*, *23*, 85–88, 1996b.

Santee, M. L., et al., Interhemispheric differences in polar stratospheric HNO_3, H_2O, ClO, and O_3, *Science*, *267*, 849–852, 1995.

Solomon, S., Progress towards a quantitative understanding of Antarctic ozone depletion, *Nature*, *347*, 347–354, 1990.

Waters, J. W., et al., Stratospheric ClO and ozone from the Microwave Limb Sounder on the Upper Atmosphere Research Satellite, *Nature*, *362*, 597–602, 1993a.

Waters, J. W., L. Froidevaux, G. L. Manney, W. G. Read, and L. S. Elson, MLS Observations of lower stratospheric ClO and O_3 in the 1992 southern hemisphere winter, *Geophys. Res. Lett.*, *20*, 1219–1222, 1993b.

Waters, J. W., et al., UARS MLS observations of lower stratospheric ClO in the 1992–93 and 1993–94 Arctic winter vortices, *Geophys. Res. Lett.*, *22*, 823–826, 1995.

Waters, J. W., et al., Validation of UARS Microwave Limb Sounder ClO measurements, *J. Geophys. Res.*, *101*, 10,091–10,127, 1996.

World Meteorological Organization (WMO), Scientific assessment of ozone depletion: 1994, *WMO Rep. 37*, Global Ozone Res. and Monit. Proj., Geneva, 1995.

L. Froidevaux, G. L. Manney, W. G. Read, M. L. Santee (mls@camel.jpl.nasa.gov), and J. W. Waters, Jet Propulsion Laboratory, Mail Stop 183–701, 4800 Oak Grove Drive, Pasadena, CA 91109.

(received May 29, 1996; revised July 30, 1996; accepted August 5, 1996.)